Temperature and pressure effects on the electrochemical CO2 reduction

Vos, R.E.

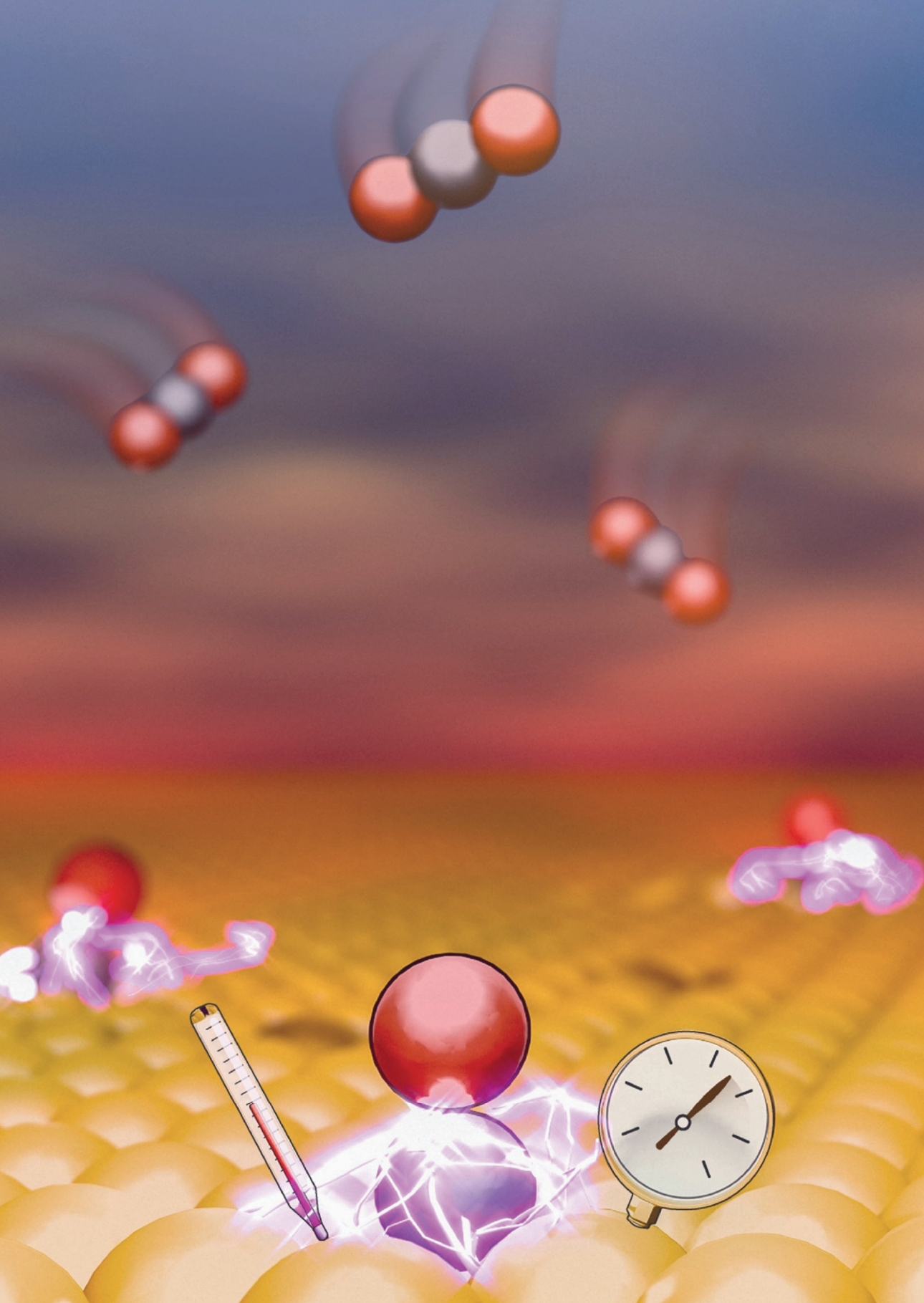

8

Screening of various metals for electrochemical CO_2 reduction at elevated temperatures and pressures

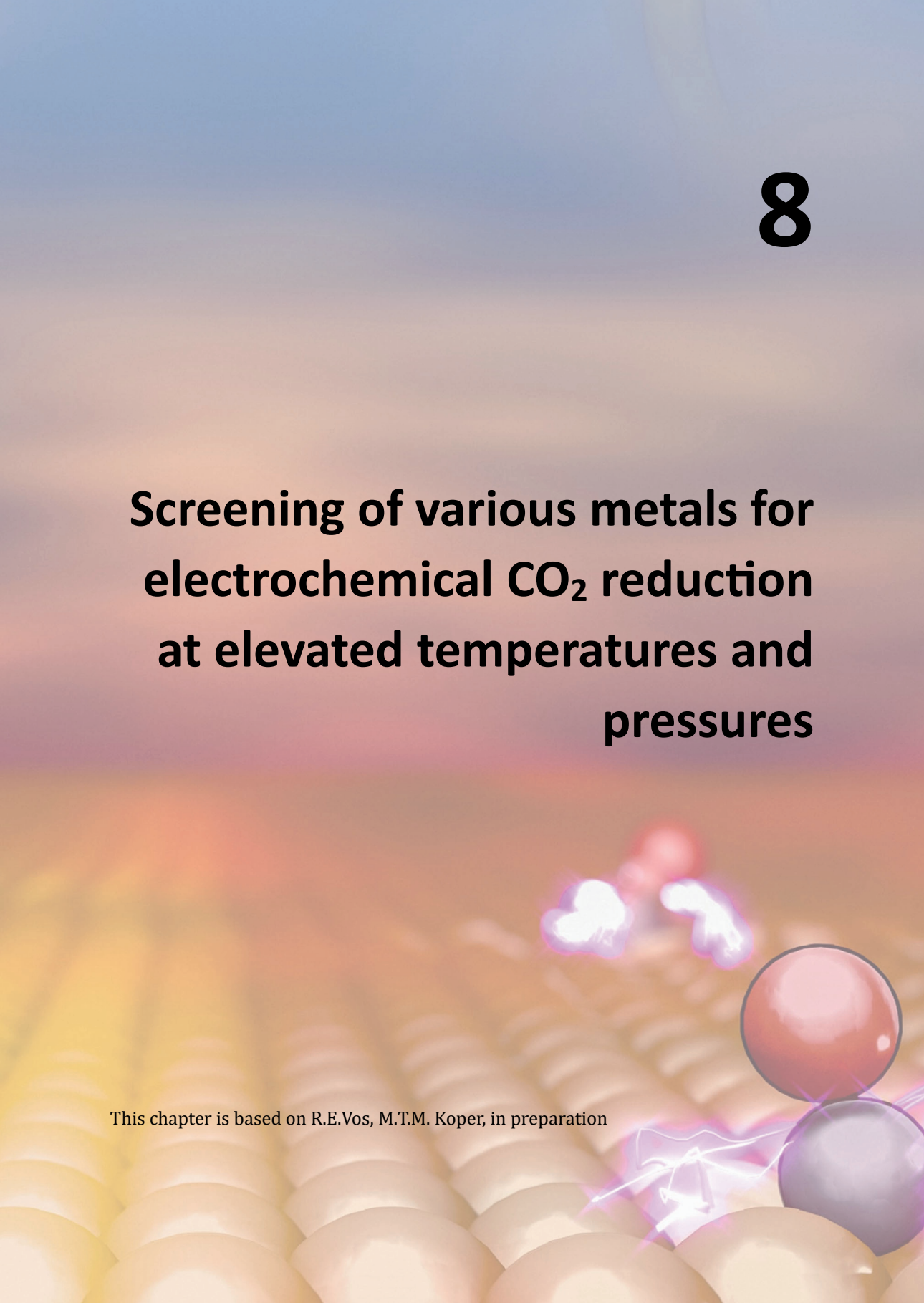

This chapter is based on R.E.Vos, M.T.M. Koper, in preparation

Abstract

Traditionally, the catalysts for the electrochemical CO_2 reduction reaction (CO2RR) have been categorized in 4 groups, producing mainly H_2, CO, HCOOH or C2+ products. However, this categorization is based on experiments at ambient conditions. With our high-pressure, high-temperature electrochemical cell, we are able to perform CO_2 reduction at vastly different conditions. In this study we have screened 20 metal catalysts for their ability to perform CO_2 reduction at conditions up to 30 bar and 100 °C in aqueous electrolyte. We show that catalysts that have average activity at ambient conditions, can reach near 100% efficiency for CO2RR at 30 bar and maintain this at high temperatures. Both temperature and pressure can increase the CO2RR activity significantly. However, if a catalyst does not perform CO2RR at ambient conditions, increasing pressure and temperature will only increase CO2RR selectivity to maximum 30%. Nevertheless, some of these inferior CO2RR catalysts do show interesting products beyond CO and HCOOH, such as long chain hydrocarbons and methanol.

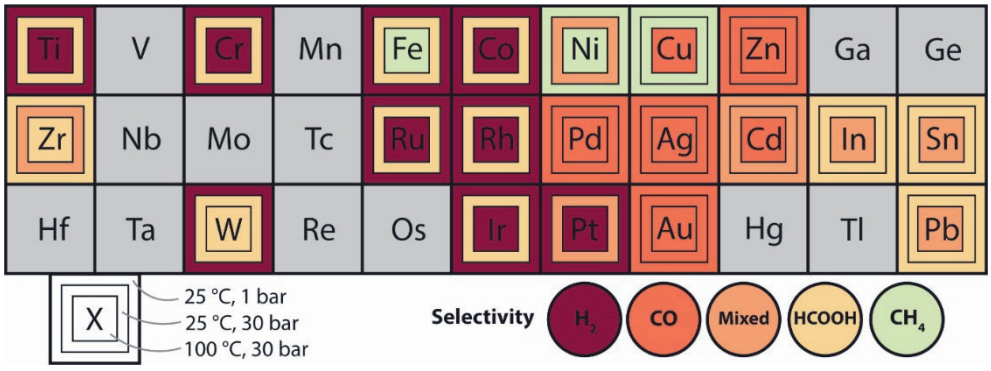

8.1 Introduction

The electrochemical CO_2 reduction reaction (CO2RR) is an interesting reaction to study as it could produce sustainable fuels and feedstocks for the chemical industry, and in this way fits in a sustainable green society [1–4]. Metals can be excellent catalysts for this reaction and these catalysts are traditionally classified in 4 groups [5,6]; metals as Au, Ag an Zn produce mainly CO from CO_2, metals such as Pb, Sn and In form mainly HCOOH, and Cu is the special one being able to form C-C bonds and produce products such as ethanol and ethylene. Lastly, there are metals such as Pt, Pd and Ni which are more active for the competing hydrogen evolution reaction (HER). This classification is based on data at ambient conditions, but these are probably not the typical conditions under industrial applications. Therefore, it is important to study the effect of temperature and pressure on a wide range of metal catalysts for CO2RR.

Temperature has been shown to increase the selectivity towards CO2RR compared to HER on Au, Cu and Ni at ambient pressures [7–9]. Often an optimal temperature is found, as too high temperatures can lead to too low CO_2 concentrations in electrolyte, or to instability of the metal catalyst. Temperature not only influences the selectivity but also significantly enhances the activity, both of CO2RR and HER. These trends are not only observed in H-cell configurations, but also in GDE setups, with catalyst such as Ag[10] and Sn[11].

Pressure can also significantly influence the CO_2 reduction reaction. Hara et al.[12] showed that even catalysts which at ambient conditions mainly produce H_2, such as Zr and Pt, could produce some CO2RR products at 30 bar. Also for catalysts of the other categories, pressure can improve the activity and selectivity towards CO or HCOOH[13,14]. Moreover, elevated pressures could even lead to new products, for example hydrocarbons on Ni[15], oxygenates on Ag[16] and 2-propanol on Cu[17].

Recently, we have developed a high-pressure, high-temperature electrochemical cell, which can be used to study the CO2RR at both high temperature and high pressure simultaneously[18]. This combination gives us the opportunity to study this reaction under new experimental conditions and perform experiments at or above 100 °C in aqueous electrolyte. The combination of elevated pressure and temperature can improve both selectivity and activity, as has been shown for CO on Au[18] and for ethylene on Cu. Moreover, at high temperatures and pressures new reaction pathways can be open up, such as the chain growth mechanism for C-C coupling on Cu as shown in the previous chapter.

In this study, we use our high-pressure high-temperature electrochemical cell to screen 20 metal catalysts for CO2RR. The effect of pressure and the combined

effect of high temperature and pressure on these metals is studied to establish if poor CO2RR catalysts can become decent, and if decent catalysts can become excellent. We study how selectivity and activity changes with experimental conditions and if new products are produced. We show that elevated pressures can inhibit HER significantly and CO2RR can reach almost 100% FE, even at 100 °C. Although traditional HER catalysts do not reach very high FEs for CO2RR, even at high pressures, some of them do produce interesting products such as long chain hydrocarbons and methanol. This study shows what is possible and which interesting directions exist to further understand electrochemical CO_2 reduction at high temperatures and pressures in aqueous systems.

8.2 Experimental

8.2.1 Chemicals

The 0.1 M electrolyte was made from $KHCO_3$ (99.95%, Sigma-Aldrich) with Milli-Q water (≥18.2 MΩcm, TOC < 5 ppb) and stored with Chelex (100 sodium form, Sigma-Aldrich) to clean the electrolyte from any metal impurities.[19] H_2SO_4 (95-98%, Sigma-Aldrich), H_2O_2 (35%, Merck) and $KMnO_4$ (99%, Sigma-Aldrich) were utilized to clean the cells. CO_2 (4.5 purity, Linde) was used for purging the electrolyte.

8.2.2 HP cell setup

An adapted high pressure, high temperature cell from Parr instruments with an Ag/AgCl reference from Corr instruments was used in this study. More details on the cell have been described before in a recent paper[18]. The cell was designed to work up to 140 bar and 200 ^{0}C and was used in semi-continuous mode where CO_2 was constantly purged through the cell with a flow rate of 150 ml/min. After going through a condenser coupled to a cooler (Cool-Care, Van der Heijden Labortechnik GMbH) to keep all volatile products in the liquid phase in the setup, the outlet gas was analyzed every 6 min with a Micro-GC from Agilent with two TCD detectors. A combination of a MS6A and CP-PORABOND Q column was used to detect H_2, CO and CH_4 and a Al_2O_3 column was used to detect the C2 and C3 hydrocarbons. The pressure in the cell was maintained by controlling both the inlet and outlet flow with flow controllers (SLA5850, Brooks Instruments). The temperature was controlled with an electric heating mantle. A homemade two-compartment PEEK cup was used inside the stainless steel chamber and all metal parts from the thermocouple and reference electrode were covered by Teflon tape. Moreover, the lid of the vessel was covered with Viton rubber to prevent any contamination from the stainless steel.

8.2.3 Electrochemical experiments

The homemade PEEK cup was cleaned prior to experiments by storing in permanganate solution overnight (0.5 M H_2SO_4, 1g/L $KMnO_4$). Afterwards, the cell was washed, cleaned in diluted mixture of H_2SO_4 and H_2O_2 to remove any traces of MnO_4 and MnO_2, washed again and boiled three times with Milli-Q water. As working electrodes, 1mm thick wires were used. Table G.1 gives an overview of the supplier and the purity of the wires. The wires were used as received, except for the Cu, which was electropolished in 85% H_3PO_4 (Suprapure, Merck) by applying +3 V versus a graphite counter electrode for 20 s before the experiment. The working electrode was separated from a DSA counter electrode (Magneto) with a PiperION membrane (Versogen)[20,21]. The experiments were performed with a Gamry Interface 1010B potentiostat and current interrupt[22] was used to correct for the Ohmic drop. Experiments were performed for 60 minutes at constant potential, in principle -1.5 V vs SHE. Gaseous products were determined every 6 min with GC as described above, while liquid products were determined afterwards by sampling the 65 ml catholyte and analyzing this using high performance liquid chromatography (HPLC, Shimadzu) with an Aminex HPX-87H column (Bio-rad). Methanol was not detected with HPLC but using a liquid GC with a SH-I-MS column (Nexis GC 2030 with AOC-30i autosampler, Shimadzu). During experiments the pressure was maintained within an error of 0.1 bar, while temperature was maintained within an error of 2 °C. Before reaching the conditions used for the experiment (which could take up to an hour), the working electrode was always under potential control at a potential of -0.8 V vs Ag/AgCl. Due to time restraints, individual experiments have not been repeated and no error bars are plotted.

8.2.4 Reference electrode corrections

In this study, all potentials are reported vs SHE(T). During experiments, a high pressure Ag/AgCl electrode (Ultradeg, 0.1 M KCl, Corr Instruments) was used as a reference electrode. However, with changing temperature, one should make several corrections to convert the potential from Ag/AgCl to SHE as we described previously (REF to HP Cu paper). The Nernst equation is used to determine the shift of the Ag/AgCl reference electrode against SHE:

$$E_{Ag/AgCl} = E^0_{Ag/AgCl}(T) - \frac{\ln(10) * RT}{nF} * \log\left(a_{Cl^-}(T)\right) \qquad (8.1)$$

with E^0 the standard potential, R the gas constant, T the temperature, n the number of electrons, F Faradays constant and a_{Cl} the activity of the chloride anion. The standard potential of Ag/AgCl is a function of temperature and can be calculated using the following formula[23]:

$$E^0_{Ag/AgCl}(T) = -0.111658 + 0.011134 * T - 0.001757268 * T * \ln(T) \qquad (8.2)$$

The temperature dependence of the activity of the chloride ions can be determined from a formula from Bogaerts et al.[24] :

$$a_{Cl^-}(T) = exp\left[\log\left(a_{Cl^-}(25\,^\circ C)\right) - \frac{\sqrt{I_{Cl^-}}}{1+\sqrt{I_{Cl^-}}} * \left(A_\gamma^T - A_\gamma^{25\,^\circ C}\right)\right] \qquad (8.3)$$

where a_{Cl^-} is the activity of the chloride at room temperature[25] I_{Cl} is the ionic strength and A_γ is the Debye-Huckel parameter[24]

With these formulas, the shift between an Ag/AgCl reference and SHE could be determined at different temperatures, as shown in Table G.2. The potential could not be reported in RHE as the pH should be known to convert SHE to RHE. However, it is impossible to measure the exact pH of the electrolyte at elevated CO_2 pressures and temperatures.

8.3 Results

8.3.1 Selective screening

We have performed experiments on a selection of metal catalysts for CO2RR at elevated pressures and temperatures. Because our setup opens up the parameter space for both pressure and temperature, many combinations of conditions are possible, especially when electrolyte composition and potential are also taken into account. Therefore, in this study we have limited the parameter space and all experiments are in principle performed in 0.1 M $KHCO_3$ at -1.5 V vs SHE, which is equivalent to -1.1 V vs RHE at ambient conditions. Moreover, we study six temperature and pressure combinations for seven main metal catalysts. Ambient conditions are studied as reference point, room temperature and 30 bar to study the effect of pressure, and to be able to compare with known literature. The effect of temperature is studied at 50 and 100 °C, at 30 bar, and to observe the effect of pressure at these temperatures also experiments at 5 bar were performed. Figure 8.1 shows part of the periodic table and the main CO2RR products of these metals at ambient conditions [5,6]. We have chosen to study Cu, as it is the only one making products beyond CO. Zn and Ag are studied as typical CO producing catalysts, while Cd and Sn typically make HCOOH. Ni and Pd are studied to complete the set with catalysts that at ambient conditions produce mainly H_2. With the exception of Sn, the studied metals all surround Cu as we expect this gives the highest chance to observe products beyond CO when the temperature and pressure are altered. Besides these 7 metals, 16 other metal catalysts such as Au, Pb, Pt and Fe are studied as well, although in less detail, in Figure 8.4.

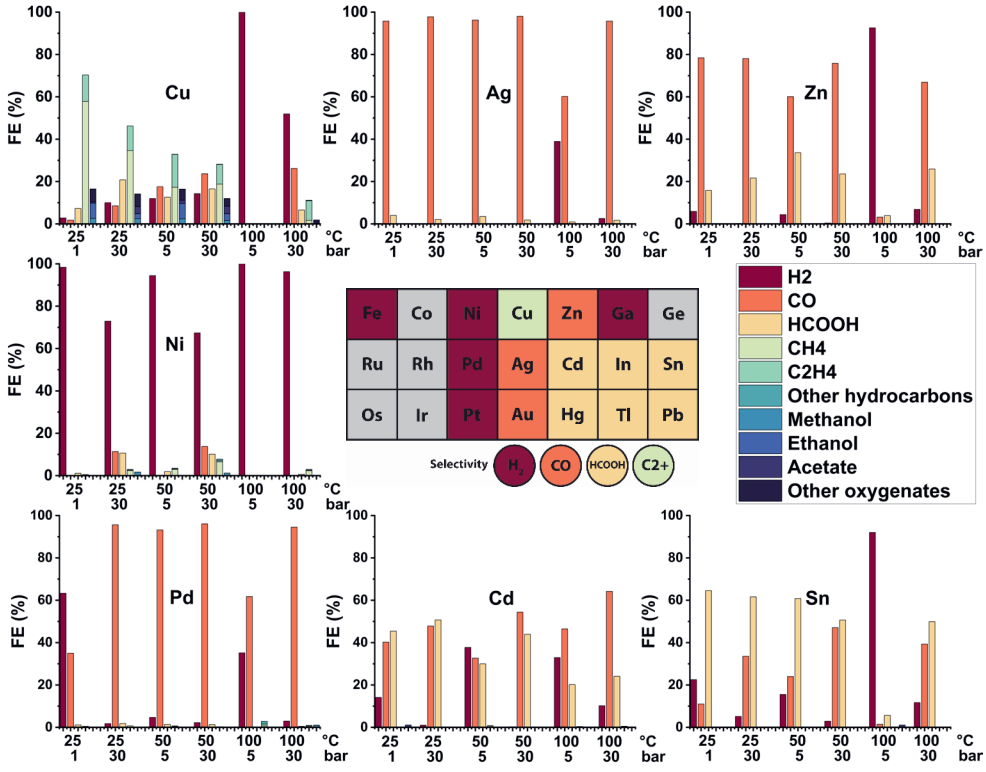

Figure 8.1 Faradaic efficiency at six different conditions for Cu, Ag, Zn, Ni, Pd, Cd and Sn at -1.5 V vs SHE in 0.1 M $KHCO_3$. These metals were studied as they represent the different groups of metals as shown in the Periodic Table in the middle(REF); hydrogen as main product, CO or HCOOH and Cu as catalyst able to make C2+ products.

Figure 8.1 shows the Faradaic efficiency towards the main products at the different pressure and temperature combinations for Cu, Ag, Zn, Ni, Pd, Cd and Sn. The competing hydrogen evolution reaction can be significantly suppressed on most of these metals at elevated pressures. Ag, Zn, Cd and even Pd show hardly any H_2 at 30 bar at room temperature, while Cu and Sn only produce up to 10%. Only Ni still produces significantly amounts of H_2 at these conditions, although with 70% also significantly less than the almost 100% at ambient conditions. With increasing temperature up to 50 °C, the HER efficiency remains low. At 100 °C, H_2 selectivity rises slightly for most metals, although only very significantly for Cu and Ni. At elevated temperatures, high pressures are needed to keep HER suppressed as at 5 bar the H_2 selectivity increases again, especially at 100 °C, where it starts to dominate not only on Ni, but also on Cu, Sn and Zn. The dominance of hydrogen at 100 °C and 5 bar is not simply due to low CO_2 solubility, as at this condition the CO_2

solubility is higher than at ambient conditions but CO_2 reduction performance is worse.

Low efficiency towards H_2 means that most current is used to make CO2RR products. While Pd and Ag are very selective and produce almost 100% CO at elevated pressures, Cd, Sn and Zn produce both CO and HCOOH. While at ambient conditions Zn and Sn produce mainly the product they are expected to produce (CO and HCOOH respectively)[5,6], Cd already produces a mixture of CO and HCOOH at these conditions even though it is expected to produce mainly HCOOH. How the ratio between CO and HCOOH changes in general with pressure and temperature, will be discussed in more detail in section 8.3.3. It is interesting to notice that when almost 100% efficiency towards CO2RR is reached, it is either towards CO (for Pd and Ag) or towards a mixture of CO and HCOOH (for Cd, Sn and Zn), but never only towards HCOOH. In the literature, HCOOH has been observed as the dominating CO2RR product at elevated pressures, even reaching efficiencies above 90% [26]. However, the FE towards HCOOH strongly depends on potential[26], so it might be that we are not at the optimal potential for the formation of HCOOH.

At high pressure and low to medium temperatures, Ni is able to perform CO2RR in significant amounts and it produces a mixture of products; not only CO and HCOOH, but also hydrocarbons. These hydrocarbons are mainly methane, but also ethane, ethylene, propene and trace amounts of C4 products are observed. The formation of ethane and propene indicates that a chain growth mechanism is active, as has been shown before for Ni [9,27]. Interestingly, not only Ni produces these longer chain hydrocarbons but also Cu and Pd produce some longer chain hydrocarbons at elevated temperatures. Cu produces a mixture of products, as expected. At ambient conditions, mainly hydrocarbons are produced on Cu, but the selectivity towards these decrease with both temperature and pressure and at 50 °C and 30 bar there is a relatively equal mixture of all product categories. These trends fit with the trends observed before in a more detailed study to the combined effect of pressure and temperature on Cu in Chapter 7. The only metals that are able to produce oxygenates in detectable amounts besides Cu are again Ni and Pd. Both metals can produce methanol, but only under very specific conditions. On Pd, a trace of acetate has been detected at 100 °C and 30 bar. From literature it is known that Ag can produce oxygenates at elevated CO pressures [16], but we did not observe any during CO2RR. Besides that we use CO_2 and not CO, these rates are also so small that it would not lead to any significant amount of FE for these oxygenates. Moreover, Kuhl et al.[28] have shown that several metals can produce methane and methanol, even at ambient conditions, such as Zn, Ag and Au. However, this was only observed at very specific potentials and with very low activity.

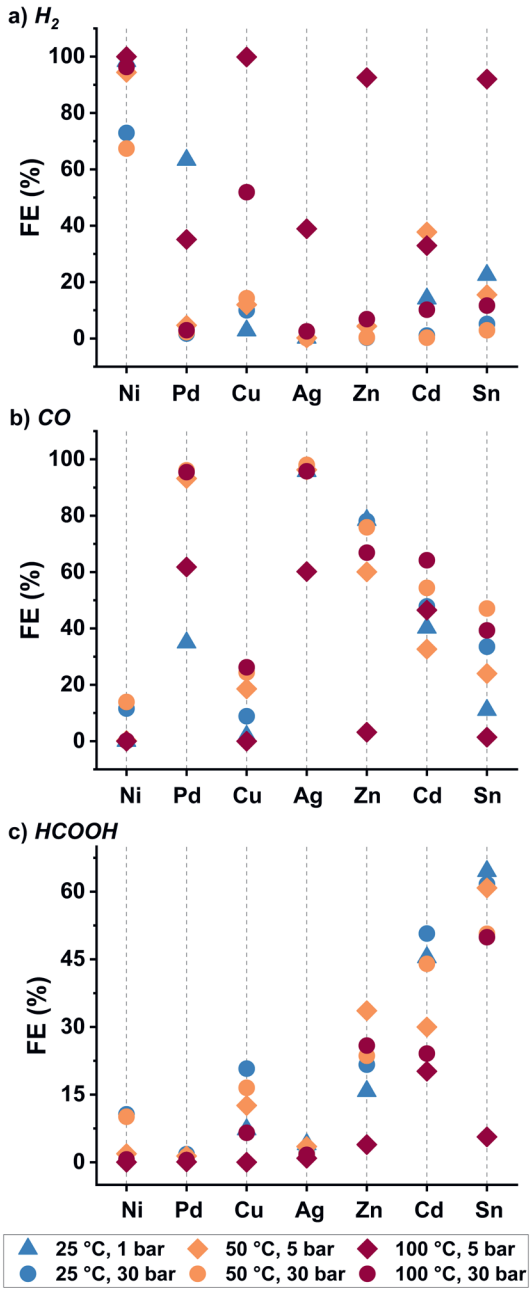

Figure 8.2 Faradaic efficiency for a) hydrogen b) carbon monoxide and c) formic acid at six different conditions for Cu, Ag, Zn, Ni, Pd, Cd and Sn at -1.5 V vs SHE in 0.1 M $KHCO_3$

Figure 8.2 shows the same data of Figure 8.1, but plotted in a different way, to gain further insights in the trends. It shows how the selectivity towards the main products CO, HCOOH and H_2 changes with the different conditions on the different metal catalysts. Figure 8.2a gives an even more pronounced illustration than Figure 8.1 how H_2 selectivity is influenced by pressure and temperature. H_2 can be almost completely suppressed with increasing pressure except on Ni. This suppressing effect can be maintained with increasing temperature. However at high temperatures, elevated pressures are needed to maintain high CO2RR selectivity because high FE towards H_2 are mainly observed at 100 °C and 5 bar.

Pd and Ag produces CO with almost 100% FE under most conditions. Cu, Zn, Cd and Sn show more variation in the CO selectivity with temperature and pressure. On Zn, the selectivity towards CO remains fairly constant at low temperatures and only slightly decreases at 100 °C, or at the combination of elevated temperatures and low pressures. For Cu, Cd and Sn, the FE towards CO seems to increase with increasing temperature, although mainly at 30 bar. For the selectivity towards HCOOH, it is apparent that the highest efficiencies are reached at room temperature, especially for the metals known for producing formic acid. With increasing temperatures, these catalysts are becoming less selective towards HCOOH, which is similar to what has been observed before on Cu under ambient pressures [8] and on Sn and In at elevated pressures[29]. Although in general higher pressures increase the selectivity towards formic acid (for example at room temperature on Cu, Zn and Cd), in some cases higher pressure actually decreases the selectivity towards formic acid (50 °C on Zn and Sn).

Figure 8.3 shows the partial current densities which accompany the selectivities of Figure 8.1 and 8.2. Note the breaks in the y-axis. These breaks are necessary to be able to spot the details at low current densities, while also showing the few extreme cases. Especially for H_2, the partial current densities can go to very high values at high temperatures, mainly in combination with low pressure. In these conditions, some metals are not very stable and produce large amounts of H_2. To illustrate this, the current vs time for Cu and Ni at high temperature and low pressure have been plotted in Figure G.3. For all products, the highest current densities are observed at 100 °C. For the CO2RR products, the effect of pressure on the partial current densities is also apparent as the highest current densities are reached at elevated pressures. Even though the FE towards HCOOH decreases often with temperature as discussed above, the partial current density still increases significantly. When the metal catalyst is stable, increasing either pressure or temperature is an effective strategy to increase the activity of CO_2 reduction, as is illustrated for Ag, Zn and Cd in Figure G.3 and as shown before in the same setup for Au[18].

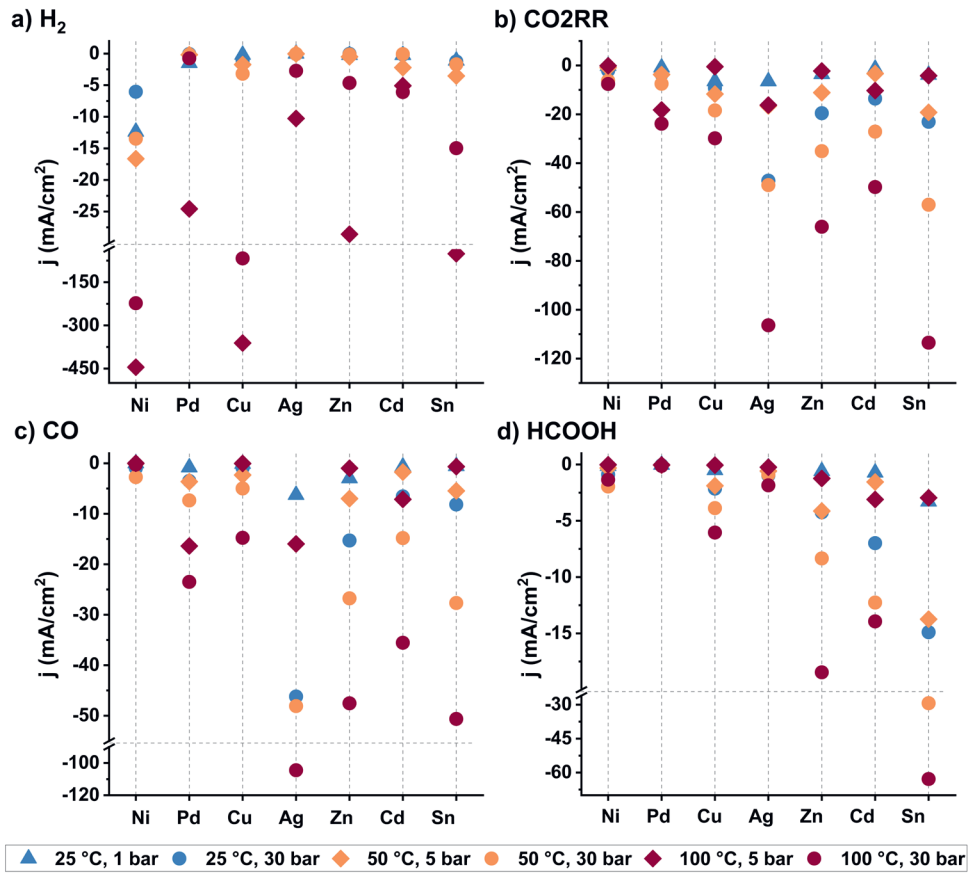

Figure 8.3 Partial current densities for a) hydrogen b) all CO2RR products c) carbon monoxide and d) formic acid at six different conditions for Cu, Ag, Zn, Ni, Pd, Cd and Sn at -1.5 V vs SHE in 0.1 M $KHCO_3$.

8.3.2 Broader screening

In the above discussion, we have studied a small selection of possible metal catalysts. However, many more metals could be studied, of which some are known to be good CO2RR catalysts at ambient conditions. However, it is also interesting to investigate the catalysts that produce mainly H_2 at ambient conditions to study if a poor CO2RR catalyst can turn into a good catalyst when the conditions, such as pressure and temperature, are optimal. Ni and Pd are examples of the this, where both significantly improve their CO2RR activity and selectivity under the right conditions. Therefore, we decided to study a larger range of metals and see what the effect of pressure and temperature is on the CO2RR. To limit the parameter space, we only study these catalysts under three conditions, namely ambient

conditions as reference point, room temperature and 30 bar to study the effect of pressure, and 100 °C and 30 bar to observe the effect of temperature. These conditions have been chosen as Figures 8.1 and 8.2 show that elevated temperature with low pressure is not a good combination for CO2RR. Moreover, the difference between 50 and 100 °C is in most cases not that significant at 30 bar, but at 100 °C some other products have been observed on Pd and Cu. Ni does show that for a poor CO2RR catalyst, 100 °C might be too high and leads to mainly H_2, but in that case the 50 °C does not provide much more insight than the case at 25 °C and 30 bar. Therefore, it was decided to study 100 °C and not 50 °C for this broader screening.

Figure 8.4 shows the effect of pressure and temperature on the CO2RR on Ti, Zr, Cr, W, Fe, Ru, Co, Rh, Ir, Pt, Au, In and Pb. The last three metals are known to be good catalysts at ambient conditions for CO2RR, while the others mainly produce H_2 at these conditions. While Au, In and Pb can reach very high CO2RR selectivities at high pressures both at 25 and 100 °C, the other catalysts remain producing mostly hydrogen at all conditions. Thus, a poor CO2RR catalyst at ambient conditions can not become a good catalyst by simply changing the pressure and temperature, as further illustrated in Figure 8.5.

In Figure 8.5 we plot the Faradaic efficiency towards CO2RR at different conditions against each other to clearly illustrate how these conditions improve the CO2RR selectivity (compared to HER). For example, Figure 8.5a show the effect of pressure on the CO2RR selectivity by plotting the FE for CO2RR at 30 bar and 25 °C vs the FE for CO2RR at 1 bar and 25 °C. This Figure shows that a poor CO2RR catalyst at ambient conditions (on the far left side of the graph) cannot be turned in a good one by increasing the pressure (on the top side of the graph). A poor catalyst can be turned in a slightly better catalyst at best, as shown in Figure 8.5b, where none of the catalysts reaches much more than 25% FE towards CO2RR. However, a reasonable CO2RR catalyst with FE toward CO2RR as low as 30% at ambient conditions (at these potentials), such as Au, In and Pd, can become a very good catalyst with less than 10% FE for HER at elevated pressures (Figure 8.5a), even at high temperatures (Figure 8.5c and d).

Even though the poor CO2RR catalysts do not have high CO2RR selectivity, there are still some interesting observation to be made from Figure 8.4. For these poor CO2RR catalysts, the main product at high T and p is HCOOH. Pt and Zr are exceptions, as they produce also significant amounts of CO. Coincidently, from all the poor CO2RR catalysts, Pt and Zr also produce the least hydrogen at elevated pressures. Moreover, we observe that some of these catalysts are able to produce long chain hydrocarbons and methanol, which we will discuss in more detail in section 8.3.3.

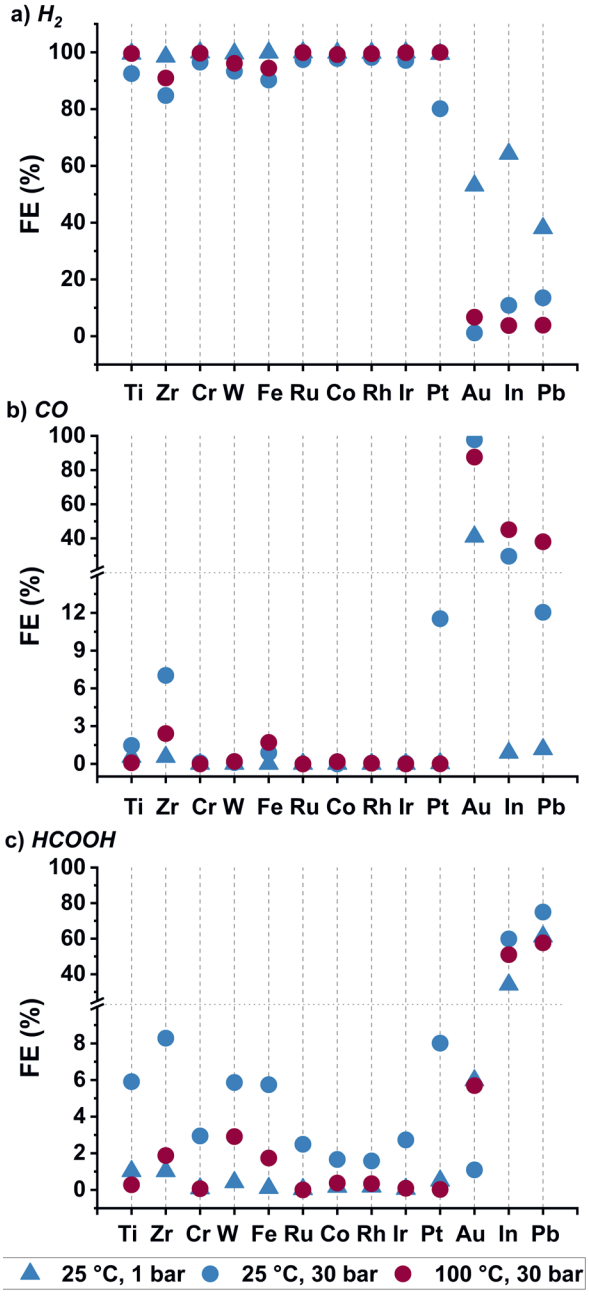

Figure 8.4 Faradaic efficiency for a) hydrogen b) carbon monoxide and c) formic acid under the three main conditions (ambient, high pressure, high temperature and pressure) for a variety of metal catalysts at -1.5 V vs SHE in 0.1 M $KHCO_3$.

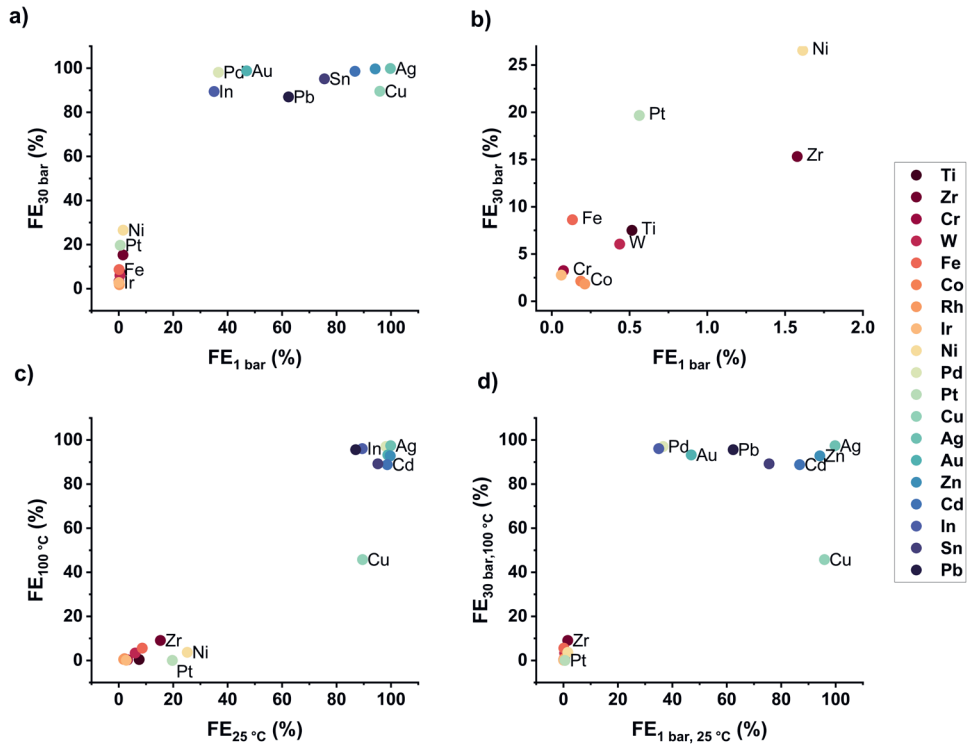

Figure 8.5 The Faradaic efficiency towards CO2RR plotted against different conditions as an illustration of the improvement (p,T) conditions can have. For example, a) shows the effect of pressure at room temperature, where medium CO2RR catalysts at ambient conditions can become very good at high pressure, but poor catalysts at ambient conditions at best become mediocre. b) is a zoomed-in version of a) showing the poor CO2RR catalysts. c) shows the effect of temperature at 30 bar and d) shows the combined effect of pressure and temperature.

The poor CO2RR catalysts at ambient conditions do not become very active at elevated pressures, not even at room temperature. This is different than observed before by Hara et al.[12] as they observed reasonably high FE for CO2RR on metals as Zr (40%), Pt (57%) and Rh (80.8%). Figure G.4 compares our results with the results of Hara et al. and Figure G.4c indeed shows that for the poor CO2RR catalysts, we observe significantly more H_2 than Hara et al. However, for some of the good CO2RR catalysts, we observe much more CO than Hara et al. There is not a systematic difference between the studies of Hara et al. and this study for H_2 and CO, although we observed in general less HCOOH for the most active HCOOH

producing metals as Pb and Sn. Both studies were performed in the same electrolyte, at similar pressures and temperatures, but a key difference is that we employ constant potential measurements while Hara et al. employ constant current measurements. Therefore, the potential in their experiments can be very different depending on the metal studied, and this might explain the different results between the two studies. A comparison between the study of Hori[5] and this study in Figure G.5 leads to a similar observations. However, the HCOOH efficiency in the study of both Hara and Hori is exceptionally high and was not reached in many other studies[30–33], or only at certain conditions of potential, electrode roughness and temperature [26,34,35]. Therefore, we expect that under (slightly) different conditions, near 100% FE towards HCOOH should also be achievable in our setup.

8.3.3 Discussion activity, stability, selectivity

Figure G.6 shows that the activity towards CO2RR increases with both increasing temperature and pressures. This is similar to what we have shown before in a more detailed study on Au using this setup [18]. Only under conditions where CO_2 availability becomes limited, or when the catalyst becomes unstable, this relationship does not hold. In Figure G.6 this is most clearly illustrated by the data points at 100 °C and 5 bar, which are often lower than expected based on the other results. Moreover, Figure G.3 illustrates that not all metals are stable under the conditions applied in this study. Especially at high temperatures and low CO_2 pressures, we observe instabilities, which are illustrated by the increase of the total current due to the increase in HER selectivity in time. This instability also influences the product distribution, as can be seen in Figure 8.5c and d, because the instabilities lead to more HER and relatively less CO2RR. Therefore, while all other reasonable CO2RR catalyst cluster together in the top right corner of Figure 8.5c, Cu is the only one significant below that. This means that for most CO2RR catalyst, they produce very little H_2 when the pressure is increased to 30 bar and this remains the case even at 100 °C because they are stable. However, Cu becomes unstable at these temperatures and as a consequence starts producing significant amounts of H_2, which lowers the CO2RR selectivity and makes Cu and outlier in Figure 8.5c.

The selectivity of the reaction and especially the competition between the main products CO and HCOOH is analyzed in more detail in Figures G.8, G.9 and G.10. Figure G.8 shows the selectivity towards hydrogen, formic acid and CO plotted against the H* binding energy calculated by Bagger et al.[6] They argue that H* binding energy is the key descriptor predicting the main product, although recently it has been argued that the crystal lattice also works as descriptor[36]. In these plots, the different classes of CO2RR catalysts can clearly be seen and seem to reasonably

hold even at these different conditions. However, there are some exceptions of which Pd is a clear example. Based on its *H energy, Pd is expected to produce mainly H_2, as it was classified before by Bagger et al.[6] However, we observed that HER can be suppressed almost entirely on Pd, maybe because one should consider a palladium hydride surface instead[37–41]. Also Ni and Pt move away from the cluster on top, but only at elevated pressures. Even though the H* binding energy still seems a reasonable descriptor even at high temperature and pressure, the difference between the CO and HCOOH producing metals becomes less sharp and more gradual in these conditions. Zn, which is classified as producing CO, makes relatively less CO by increasing pressure and temperature while Cd and the HCOOH-producing metal move in opposite direction and seem to produce more CO with increasing pressure and temperature. Figure G.8 illustrates that with increasing pressure the Faradaic efficiency towards HCOOH can either increase or decrease and this seems to depend on the *H binding energy. For metals known for producing HCOOH, the FE decreases with increasing temperature, while the metals with stronger *H binding energies slightly increase their selectivity towards HCOOH. As formic acid and CO are the main CO2RR products for most catalysts, it is interesting to see how the ratio between these products changes with changing operation conditions. Figure G.9 illustrates that both with increasing pressure and temperature in most cases the CO selectivity increases more than the HCOOH selectivity, at least for the potential and electrolyte used here.

Figure G.10 shows that some metal catalysts (Fe, Co, Ni, Pd, Cu) have the ability to make hydrocarbons at high pressures, sometimes only in combination with high temperatures (Zr and Cd). Various metals show some methane production and others show even longer hydrocarbons. These efficiencies are very low, but not uninteresting as this shows that these metals are capable of producing C2+ products and this is not limited to Cu only. Because no other liquid C2+ products are detected at any other metal than Cu (except for trace of acetate on Pd) and because these metals are able to produce longer hydrocarbons, we expect that these metals perform C-C coupling via a chain growth mechanism instead of the traditional CO dimerization mechanism. Maybe not coincidentally, some of the metals that perform this electrochemical chain growth mechanism are also able to do this thermocatalytically and are active for the Fischer-Tropsch reaction[42–44], such as Fe, Co and Ni, although Ru does not show the formation of hydrocarbons in this study. Also interestingly, some metals are able to produce methanol as well (Figure G.11). Fe produces methanol both at 25 and 100 °C at 30 bar, while Ni and Cu only produce it at 25 and 50 °C and Pd only at 100 °C. Curiously, the only metals that produce methanol also produce longer hydrocarbons, which could indicate that that these products share a common intermediate, such as *HCO[28,45]. Based on this, one might expect Co to also be able to form methanol, even though this was not observed in

our experiments. Moreover, Ru has shown to be active in methanol production before, but no methanol was found in these experiments. However, in the literature often RuO_2 is used instead of metallic Ru and lower overpotentials are applied[46].

8.4 Conclusion

Figure 8.6 summarizes the trends and observations of this study, showing the selectivity of all the metals studied at ambient conditions, at elevated pressure and for the combination of elevated pressure and temperature. Section G.9 contains the details how this figure was constructed. The top periodic table shows the selectivity towards CO2RR compared to HER. Increasing the CO_2 pressure can significantly improve CO2RR and intermediate CO2RR catalysts at ambient conditions can

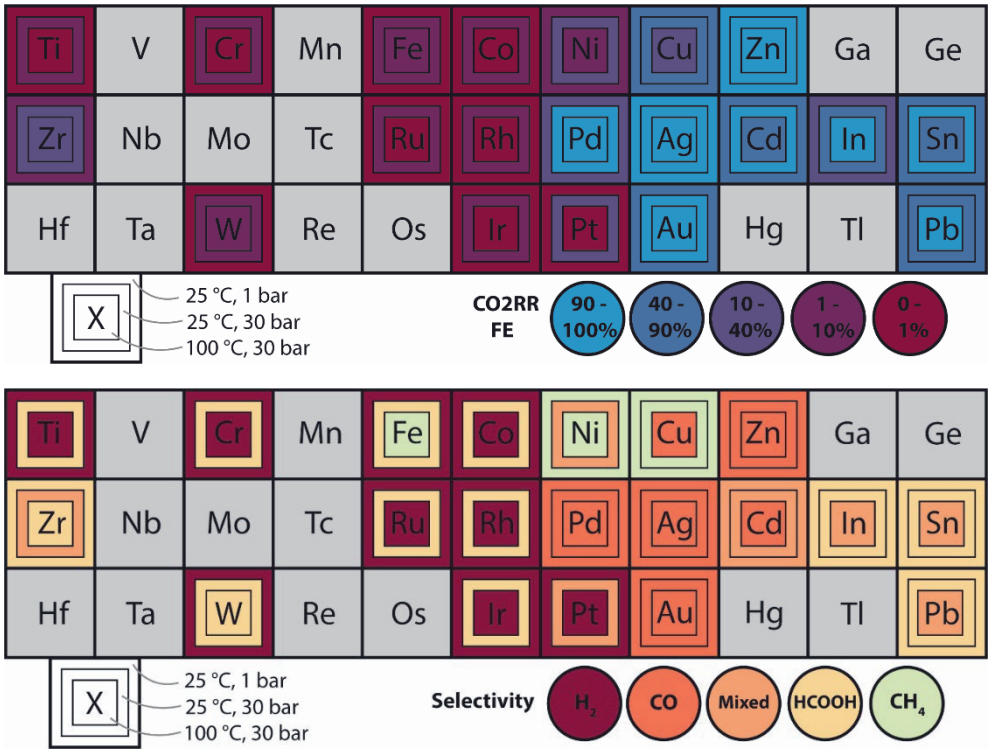

Figure 8.6 Periodic table to summarize the trends with pressure and temperature at a big variety of metal catalysts for electrochemical CO_2 reduction at -1.5 V vs SHE in 0.1 M $KHCO_3$. The upper Periodic table shows the selectivity towards CO2RR in competition with HER. The lower Periodic table shows the selectivity of the CO2RR products, unless so little is produced which leads to a red color for HER. Per metal, the outer box gives shows the results at ambient conditions, the middle box at high pressure and the inner box at high pressure and temperature.

become very good as HER is significantly suppressed by increasing pressure. The CO producing metals can reach very high FE with increasing pressure, even at 100 °C, while for the HCOOH producing catalysts, this high efficiency is reached at high pressures but at different temperatures depending on the catalyst. The left side of the periodic table stays more red and only at elevated pressures Faradaic efficiencies for CO2RR above 1% can be reached, although hardly ever exceeding 10%. The bottom periodic table shows the product distribution of the CO_2 reduction reaction. It can be seen that the CO producing metals always keep producing CO, while Cu and the HCOOH producing metals produce relatively more CO at elevated temperatures. The poor CO2RR catalysts produce mainly HCOOH as CO2RR product at high pressures and low temperatures. Cu is not the only metal able to produce hydrocarbons, as also Ni and Fe can produce them in significant amounts under the high pressures and temperatures.

This study has screened various metals as electrocatalysts for CO_2 reduction and specifically looked at the effect of temperature and pressure. Potential and electrolyte were kept constant during all experiments, because otherwise the parameter space would be too large. However, these parameters can have significant influence on catalyst performance [26,34,47–50]. Therefore, this screening study gives first insights, but further in-depth studies are needed in which the effect of potential and electrolyte are studied on selected catalysts. Moreover, we only studied six temperature-and-pressure combinations. Medium pressures of 10-20 bar and medium temperatures of 50-75 °C may still yield deviating results. This study therefore gives guidance in deciding future experiments. The most interesting catalysts to study for CO2RR appear to be the known catalysts as Cu, Ag and Zn, but also Pd, Ni, Fe, Zr and Pt, especially at elevated pressures and temperatures. Beyond the pure metal catalysts, these metals could also be studied as carbides, nitrides and phosphides for example [9,27,51,52]. Moreover, combining these metals in metal alloys could lead to new results and improve activity or selectivity beyond the performance of a single metal [53–58].

References

1. Mertens, J. *et al.* Carbon capture and utilization: More than hiding CO_2 for some time. *Joule* vol. 7 442–449 Preprint at https://doi.org/10.1016/j.joule.2023.01.005 (2023).
2. De Luna, P. *et al.* What would it take for renewably powered electrosynthesis to displace petrochemical processes? *Science (1979)* **364**, eaav3506 (2019).
3. Alerte, T. *et al.* Scale-Dependent Techno-Economic Analysis of CO2 Capture and Electroreduction to Ethylene. *ACS Sustain Chem Eng* **11**, 15651–15662 (2023).
4. Roh, K. *et al.* Early-stage evaluation of emerging CO_2 utilization technologies at low technology readiness levels. *Green Chemistry* **22**, 3842–3859 (2020).
5. Hori, Y., Wakebe, H., Tsukamoto, T. & Koga, O. Electrocatalytic process of CO selectivity in electrochemical reduction of CO_2 at metal electrodes in aqueous media. *Electrochim Acta* **39**, 1833–1839 (1994).
6. Bagger, A., Ju, W., Varela, A. S., Strasser, P. & Rossmeisl, J. Electrochemical CO_2 Reduction: A Classification Problem. *ChemPhysChem* **18**, 3266–3273 (2017).
7. Vos, R. E. & Koper, M. T. M. The Effect of Temperature on the Cation-Promoted Electrochemical CO_2 Reduction on Gold. *ChemElectroChem* **9**, e20220023 (2022).
8. Vos, R. E. *et al.* How Temperature Affects the Selectivity of the Electrochemical CO_2 Reduction on Copper. *ACS Catal* **13**, 8080–8091 (2023).
9. Vos, R. E. & Koper, M. T. M. Nickel as Electrocatalyst for $CO_{(2)}$ Reduction: Effect of Temperature, Potential, Partial Pressure, and Electrolyte Composition. *ACS Catal* 4432–4440 (2024) doi:10.1021/acscatal.4c00009.
10. Dufek, E. J., Lister, T. E., Stone, S. G. & McIlwain, M. E. Operation of a Pressurized System for Continuous Reduction of CO 2. *J Electrochem Soc* **159**, F514–F517 (2012).
11. Löwe, A. *et al.* Influence of Temperature on the Performance of Gas Diffusion Electrodes in the CO_2 Reduction Reaction. *ChemElectroChem* **6**, 4497–4506 (2019).
12. Hara, K., Kudo, A. & Sakata, T. *Electrochemical Reduction of Carbon Dioxide under High Pressure on Various Electrodes in an Aqueous Electrolyte*. *Journal of Electroanalytical Chemistry* vol. 391 (1995).
13. Ramdin, M. *et al.* High Pressure Electrochemical Reduction of CO2 to Formic Acid/Formate: A Comparison between Bipolar Membranes and Cation Exchange Membranes. *Ind Eng Chem Res* **58**, 1834–1847 (2019).
14. Gabardo, C. M. *et al.* Combined high alkalinity and pressurization enable efficient CO2 electroreduction to CO. *Energy Environ Sci* **11**, 2531–2539 (2018).
15. Kudo, A., Nakagawa, S., Tsuneta, A. & Sakata, T. Electrochemical Reduction of High Pressure CO_2 on Ni Electrodes. *J. Electrochem. Soc* **140**, 1541–1545 (1993).
16. Raaijman, S. J., Schellekens, M. P., Corbett, P. J. & Koper, M. T. M. High-Pressure CO Electroreduction at Silver Produces Ethanol and Propanol. *Angewandte Chemie - International Edition* **60**, 21732–21736 (2021).
17. Girichandran, N., Saedy, S. & Kortlever, R. Electrochemical CO_2 reduction on a copper foam electrode at elevated pressures. *Chemical Engineering Journal* **487**, (2024).

18. da Silva, A. H. M., Vos, R. E., Schrama, R. J. C. & Koper, M. T. M. Design of a Rotating Disk Electrode setup operating under high pressure and temperature: Application to CO_2 reduction on gold. *Electrochim Acta* **498**, 144612 (2024).
19. Wuttig, A. & Surendranath, Y. Impurity Ion Complexation Enhances Carbon Dioxide Reduction Catalysis. *ACS Catal* **5**, 4479–4484 (2015).
20. Wang, J. *et al.* Poly(aryl piperidinium) membranes and ionomers for hydroxide exchange membrane fuel cells. *Nat Energy* **4**, 392–398 (2019).
21. Achrai, B. *et al.* A Direct Ammonia Fuel Cell with a KOH-Free Anode Feed Generating 180 mW cm −2 at 120 °C . *J Electrochem Soc* **167**, 134518 (2020).
22. Heenan, A. R., Hamonnet, J. & Marshall, A. T. Why Careful iR Compensation and Reporting of Electrode Potentials Are Critical for the CO_2 Reduction Reaction. *ACS Energy Lett* **7**, 2357–2361 (2022).
23. Öijerholm, J., Forsberg, S., Hermansson, H.-P. & Ullberg, M. Relation Between the SHE and the Internal Ag⁄AgCl Reference Electrode at High Temperatures. *J Electrochem Soc* **156**, P56 (2009).
24. Bogaerts, W. F. & Haute, A. A. Van. Determination of Activity Coefficients for KCl at Elevated Temperatures. *J. Electrochem. Soc.* **131**, 68–72 (1984).
25. Dash, D., Kumar, S., Mallika, C. & Mudali, U. K. New Data on Activity Coefficients of Potassium, Nitrate, and Chloride Ions in Aqueous Solutions of KNO_3 and KCl by Ion Selective Electrodes. *ISRN Chemical Engineering* **2012**, 1–5 (2012).
26. Todoroki, M., Hara, K., Kudo, A. & Sakata, T. *Electrochemical Reduction of High Pressure CO 2 at Pb, Hg and In Electrodes in an Aqueous KHCO 3 Solution*. *Journal of Electroanalytical Chemistry* vol. 394 (1995).
27. Zhou, Y. *et al.* Long-chain hydrocarbons by CO_2 electroreduction using polarized nickel catalysts. *Nat Catal* **5**, 545–554 (2022).
28. Kuhl, K. P. *et al.* Electrocatalytic Conversion of Carbon Dioxide to Methane and Methanol on Transition Metal Surfaces. *J Am Chem Soc* **136**, 14107–14113 (2014).
29. Mizuno, T. *et al.* Effect of temperature on electrochemical reduction of high-pressure CO_2 with In, Sn, and Pb electrodes. *Energy Sources* **17**, 503–508 (1995).
30. Feaster, J. T. *et al.* Understanding Selectivity for the Electrochemical Reduction of Carbon Dioxide to Formic Acid and Carbon Monoxide on Metal Electrodes. *ACS Catal* **7**, 4822–4827 (2017).
31. Pander, J. E., Baruch, M. F. & Bocarsly, A. B. Probing the Mechanism of Aqueous CO2 Reduction on Post-Transition-Metal Electrodes using ATR-IR Spectroelectrochemistry. *ACS Catal* **6**, 7824–7833 (2016).
32. Pander, J. E., Lum, J. W. J. & Yeo, B. S. The importance of morphology on the activity of lead cathodes for the reduction of carbon dioxide to formate. *J Mater Chem A Mater* **7**, 4093–4101 (2019).
33. Bitar, Z., Fecant, A., Trela-Baudot, E., Chardon-Noblat, S. & Pasquier, D. Electrocatalytic reduction of carbon dioxide on indium coated gas diffusion electrodes-Comparison with indium foil. *Appl Catal B* **189**, 172–180 (2016).

34. Hegner, R., Rosa, L. F. M. & Harnisch, F. Electrochemical CO2 reduction to formate at indium electrodes with high efficiency and selectivity in pH neutral electrolytes. *Appl Catal B* **238**, 546–556 (2018).
35. He, Z. *et al.* Electrochemically created roughened lead plate for electrochemical reduction of aqueous CO2. *Catal Commun* **72**, 38–42 (2015).
36. Christensen, O., Bagger, A. & Rossmeisl, J. The Missing Link for Electrochemical CO2 Reduction: Classification of CO vs HCOOH Selectivity via PCA, Reaction Pathways, and Coverage Analysis. *ACS Catal* **14**, 2151–2161 (2024).
37. Ohkawa, K., Hashimoto, K., Fujishima, A., Noguchi, Y. & Nakayama, S. *Electrochemical Reduction of Carbon Dioxide on Hydrogen-Storing Materials Part 1. The Effect of Hydrogen Absorption on the Electrochemical Behavior on Palladium Electrodes*. *J. Electroanal. Chem* vol. 345 (1993).
38. Guo, S. *et al.* Robust palladium hydride catalyst for electrocatalytic formate formation with high CO tolerance. *Appl Catal B* **316**, (2022).
39. Tackett, B. M., Lee, J. H. & Chen, J. G. Electrochemical Conversion of CO2to Syngas with Palladium-Based Electrocatalysts. *Acc Chem Res* **53**, 1535–1544 (2020).
40. Abdellah, A. M. *et al.* Impact of palladium/palladium hydride conversion on electrochemical CO2 reduction via in-situ transmission electron microscopy and diffraction. *Nat Commun* **15**, (2024).
41. Min, X. & Kanan, M. W. Pd-Catalyzed Electrohydrogenation of Carbon Dioxide to Formate: High Mass Activity at Low Overpotential and Identification of the Deactivation Pathway. *J Am Chem Soc* **137**, 4701–4708 (2015).
42. Jahangiri, H., Bennett, J., Mahjoubi, P., Wilson, K. & Gu, S. A review of advanced catalyst development for Fischer-Tropsch synthesis of hydrocarbons from biomass derived syn-gas. *Catalysis Science and Technology* vol. 4 2210–2229 Preprint at https://doi.org/10.1039/c4cy00327f (2014).
43. Martinelli, M., Gnanamani, M. K., LeViness, S., Jacobs, G. & Shafer, W. D. An overview of Fischer-Tropsch Synthesis: XtL processes, catalysts and reactors. *Applied Catalysis A: General* vol. 608 Preprint at https://doi.org/10.1016/j.apcata.2020.117740 (2020).
44. Arsalanfar, M., Mirzaei, A. A., Bozorgzadeh, H. R. & Samimi, A. A review of fischer-tropsch synthesis on the cobalt based catalysts. *Physical Chemistry Research* vol. 2 179–201 Preprint at https://doi.org/10.22036/pcr.2014.5786 (2014).
45. Albo, J., Alvarez-Guerra, M., Castaño, P. & Irabien, A. Towards the electrochemical conversion of carbon dioxide into methanol. *Green Chemistry* **17**, 2304–2324 (2015).
46. Popic, J. P., Avramov, M. L. & Vukovic, N. B. Reduction of carbon dioxide on ruthenium oxide and modified ruthenium oxide electrodes in 0.5 M NaHCO 3. *Journal of Electroanalyticai Chemistry* **421**, 105–110 (1997).
47. Ummireddi, A. K., Sharma, S. K. & Pala, R. G. S. Influence of tetraethylammonium cation on electrochemical CO2 reduction over Cu, Ag, Ni, and Fe surfaces. *J Catal* **406**, 213–221 (2022).
48. Pan, H., Wang, F., Zhang, Z. & Min, S. Interfacial modification of Zn foil electrode with cationic surfactants enables efficient and selective CO production from CO2 electroreduction. *Sustain Energy Fuels* **6**, 2149–2154 (2022).

49. Hatsukade, T., Kuhl, K. P., Cave, E. R., Abram, D. N. & Jaramillo, T. F. Insights into the electrocatalytic reduction of CO_2 on metallic silver surfaces. *Physical Chemistry Chemical Physics* **16**, 13814–13819 (2014).
50. Hwang, S. Y. *et al.* Electrochemical Fisher-Tropsch chemistry across transition metals: a paradigm shift in sustainable liquid fuel production. *Nano Energy* 109881 (2024) doi:10.1016/j.nanoen.2024.109881.
51. Yin, Z. *et al.* Cu3n nanocubes for selective electrochemical reduction of co2 to ethylene. *Nano Lett* 8658–8663 (2019) doi:10.1021/acs.nanolett.9b03324.
52. Handoko, A. D. *et al.* Two-Dimensional Titanium and Molybdenum Carbide MXenes as Electrocatalysts for CO2 Reduction. *iScience* **23**, (2020).
53. Jia, Y., Li, F., Fan, K. & Sun, L. Cu-based bimetallic electrocatalysts for CO2 reduction. *Advanced Powder Materials* vol. 1 Preprint at https://doi.org/10.1016/j.apmate.2021.10.003 (2022).
54. He, J., Johnson, N. J. J., Huang, A. & Berlinguette, C. P. Electrocatalytic Alloys for CO2 Reduction. *ChemSusChem* vol. 11 48–57 Preprint at https://doi.org/10.1002/cssc.201701825 (2018).
55. Mahyoub, S. A. *et al.* Rational design of low loading Pd-alloyed Ag nanocorals for high current density CO2-to-CO electroreduction at elevated pressure. *Mater Today Energy* **24**, (2022).
56. Cai, C. *et al.* Heteroatoms Induce Localization of the Electric Field and Promote a Wide Potential-Window Selectivity Towards CO in the CO2 Electroreduction. *Angewandte Chemie - International Edition* **61**, (2022).
57. Xu, X. *et al.* Pd-Decorated Cu2O-Ag Catalyst Promoting CO2 Electroreduction to C2H4 by Optimizing CO Intermediate Adsorption and Hydrogenation. *ACS Appl Mater Interfaces* **16**, 16243–16252 (2024).
58. Vos, R. E., Smaak, J. P. & Koper, M. T. M. The temperature dependence of electrochemical CO_2 reduction on Ag and CuAg alloys. *J Catal* **436**, (2024).